REAL-TIME RECONSTRUCTION OF LONGITUDINAL PHASE-SPACE DISTRIBUTION IN HADRON BEAMLINES AND SYNCHROTRONS

S. Sherstiuk*, O. Boine-Frankenheim, Technical University of Darmstadt, Darmstadt, Germany
V. Kornilov, GSI Helmholtz Centre for Heavy Ion Research, Darmstadt, Germany

Abstract

Real-time measurement and control of the longitudinal momentum spread during the beam transfer from the transfer channel (TK) into the SIS18 synchrotron is needed for the low-loss high-intensity operation. For this purpose, two Feschenko-type beam shape monitors (BSM) will be installed in TK. This will enable the single-pass measurements and real-time reconstruction. Simulations using a differentiable tracking scheme will be applied. The underlying beam dynamics model is simplified for computational efficiency, but retaining the key aspects of space-charge and beam loading effects, while providing a sufficient reconstruction accuracy.

INTRODUCTION

Knowledge of longitudinal phase space distribution properties allows operators to control particle losses and to optimize overall machine performance.

For the GSI SIS18 synchrotron [1] it is required to monitor and control the longitudinal momentum spread at injection during regular operation. Additionally, real-time control of the momentum spread should be used as a target function for automatic optimization.

The transfer channel (TK) leads the ion beams from the linear accelerator UNILAC [2] to the synchrotron SIS18. The UNILAC accelerates ions from hydrogen to uranium, in this study we consider U^{28+} ions with the reference kinetic energy 11.4 MeV/u.

TK is a 160-meter long beamline with two buncher cavities, one with a frequency of 108 MHz at the TK's beginning and the second one 57 meters further with a frequency of 36 MHz. For diagnostic purposes two beam shape monitors (BSMs) are going to be installed: one right before the first cavity ($s_0 = 0$ m) and the other one 150 meters further ($s_1 = 150$ m). A key feature of beam dynamics in this beamline is beam elongation in presence of space charge forces. Figure 1 illustrates beam rms length $\tilde{z}$ to transverse size a aspect ratio along the TK. For aspect ratios $\tilde{z}/a \gtrsim 10$ bunches can be modeled as long bunches in a conducting pipe (using the well known g-factor). In the beginning of the TK this criterion is not satisfied and therefore another approximation is needed. Vertical dashed lines mark positions of buncher cavities (green) and BSMs (red). Horizontal dashed line marks the boundary between transition and long bunch regimes.

The phase space reconstruction problem for the TK beam line at GSI can be approached as a constrained optimization problem, described by Eq. (1). The goal is to minimize the difference between bunch profile measurements and their

* sergei.sherstiuk@tu-darmstadt.de

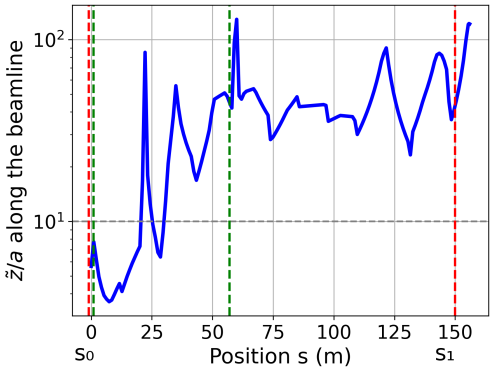

Figure 1: Longitudinal-to-transverse beam aspect ratio along the TK beamline. Vertical dashed lines mark positions of buncher cavities (green) and BSMs (red). Horizontal line marks a boundary for a long-bunch space charge regime.

counterparts from a simulation model at measurement location s_1 in the TK.

We chose the longitudinal envelope equation as a simulation model. It describes evolution of the rms bunch lengths $\tilde{z}(s) = \sqrt{\langle z^2(s)\rangle}$ where $\langle\cdot\rangle$ implies the integration over the distribution functions. Relative momentum spread $\tilde{\delta}(s_0)$ and emittance $\tilde{\varepsilon}$ are simulation parameters that have to be optimized for minimal difference between simulated length $\tilde{z}(s_1)$ and measured length $\tilde{\tilde{z}}(s)$. Length measured by the first BSM $\tilde{z}(s_0)$ is taken as a boundary condition.

The objective function is defined as a normalized squared difference between simulations $\tilde{z}(s_1)$ and measurements $\tilde{\tilde{z}}(s_1)$:

$$\min\left[\frac{1}{M}\sum_{m=1}^{M}\left(\frac{\tilde{z}_m(s_1)-\tilde{\tilde{z}}_m(s_1)}{\tilde{\tilde{z}}_m(s_1)}\right)^2\right] \tag{1}$$

where M is the number of measurements.

Search of optimal values of $\tilde{\delta}(s_0), \tilde{\varepsilon}$ is done by the gradient descent algorithm. Thus the simulation model has to support the calculation of derivatives with respect to the parameters $\tilde{\delta}(s_0), \tilde{\varepsilon}$. Another requirement is the time performance: SIS18 has a ramp-up frequency of 1 Hz and the reconstruction should be done on the same timescale in order to be used in the control room environment.

LONGITUDINAL ENVELOPE EQUATION

It was shown [3, 4] that for a group of particles and under an assumption of emittance conservation $\tilde{\varepsilon} = \sqrt{\langle z^2\rangle\langle\delta^2\rangle - \langle z\delta\rangle^2}$, rms coordinate offset $\tilde{z}$ follows the envelope equation:

$$\tilde{z}'' - \frac{\tilde{\varepsilon}^2}{\tilde{z}^3} - \frac{q\eta}{m\beta^2\gamma^3 c^2}\frac{\langle zE_{sc}\rangle + \langle zE_{rf}\rangle}{\tilde{z}} = 0. \quad (2)$$

Here prime denotes $\partial/\partial s$, E_{sc} and E_{rf} are the local space charge and external electric fields, q is particle's charge and β and γ are relativistic factors.

In drifts, where only E_{sc} is present,

$$\tilde{z}'' - \frac{\tilde{\varepsilon}^2}{\tilde{z}^3} - \frac{K_L}{5\sqrt{5}\tilde{z}^2} = 0, \quad (3)$$

here $K_L = \frac{3r_c N\eta}{2\beta^2\gamma^3}\bar{g}(s)$ is the longitudinal perveance, $r_c = \frac{q^2}{4\pi\epsilon_0 mc^2}$ is the classical particle radius, N is the number of particles in a bunch, η is the slippage factor, $\bar{g}$ is the generalized g-factor and will be discussed in the next section.

Impact of RF fields E_{rf} is represented in a thin cavity approximation. For a cavity with a wavelength λ and voltage amplitude V provides sinusoidal energy kicks, $\Delta E = qV\sin(2\pi\frac{z}{\beta\lambda})$. They translate into momentum kicks and change of envelope's derivative:

$$\Delta\tilde{z}' = \frac{qV}{m\beta^2\gamma c}\frac{\langle z\sin(2\pi\frac{z}{\beta\lambda})\rangle}{\tilde{z}} \quad (4)$$

Nonlinearities of the sine are treated by expanding it into Taylor series. In order to express higher longitudinal moments of a beam, its profile inside the cavity is assumed to be gaussian:

$$\Delta\tilde{z}' = \frac{2\pi qV}{m\beta^3\gamma\lambda c}(\tilde{z} - \frac{1}{2}(\frac{2\pi}{\beta\lambda})^2\tilde{z}^3 + \frac{1}{8}(\frac{2\pi}{\beta\lambda})^4\tilde{z}^5)) \quad (5)$$

Combination of Eq. (3) and Eq. (5) provides a model for envelope-based simulation.

SPACE CHARGE

Evolution of the bunch length along TK implies the regimes of a short bunch and a long bunch with the respect to the space-charge model [4]. We use the formalism [5] of the generalized g-factors $\bar{g}$,

$$\bar{g} = \frac{40\sqrt{5}\epsilon_0\pi\tilde{z}^3}{3qN}\frac{\langle zE_z\rangle}{\langle z^2\rangle}. \quad (6)$$

The specific values for $\bar{g}$ have been obtained from a space charge solver based on Green's function in a perfectly conducting pipe of a radius b. We calculated longitudinal electric field in the bunch rest frame along the beamline. Electric fields were calculated using a Gaussian bunch model. This gives a least-square fit for the linear field inside a bunch,

$$\bar{E}_z = \frac{3qN}{40\sqrt{5}\epsilon_0\pi\tilde{z}^3}\bar{g}z. \quad (7)$$

Eq. (2) depends on the first moment of the electric field $\langle zE_{sc}\rangle$, therefore s-dependent $\bar{g}$-factors give accurate results in the envelope model.

In the long bunch limit the $\bar{g}$-factor depends only on the transverse beam size a:

$$\lim_{\tilde{z}\to\infty}\bar{g} = 1 + 2\ln b/a. \quad (8)$$

Figure 2 compares the limit values from Eq. (8) (the red line) to the results of field-based calculations [Eq. (6), dots]. In the areas where long bunch criterion is not satisfied the logarithmic formula Eq. (8) gives an overestimation. Otherwise, $\bar{g}$ follows the evolution of the bunch transverse size. This adaptive $\bar{g}$-factor function was used in the simulations with space charge.

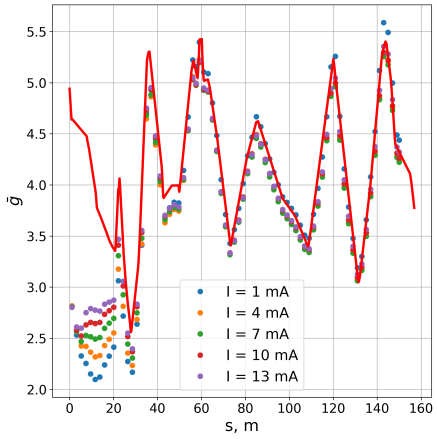

Figure 2: The generalized $\bar{g}$-factors along the TK from the exact field solver (dots) and the asymptotic values (Eq. (8), the red line).

Examples of the simulations are shown in Fig. 3. Different beam currents (giving different space-charge strength) with the fixed other settings are considered. Intense bunches can have $\tilde{z}$ up to 40% of bucket length, therefore nonlinear effects in cavities need to be considered. Space-charge forces are responsible for significant bunch length increase at high beam currents. Therefore the accurate description of the space-charge forces is needed in a reconstruction scheme .

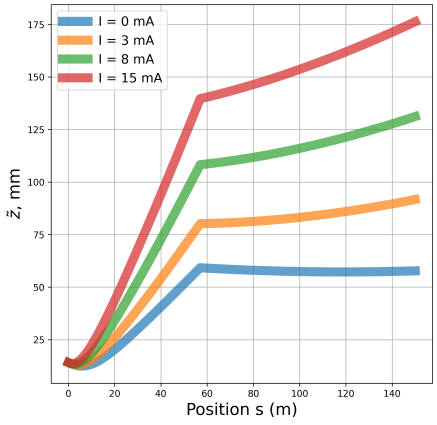

Figure 3: Bunch length evolution along TK for different beam current.

Our PyTorch implementation for the envelope model based simulations delivers the bunch length $\tilde{z}$ at the point s_1,

and also its derivatives with respect to phase space distribution parameters $\bar{\varepsilon}, \tilde{\delta}$.

PHASE SPACE RECONSTRUCTION

The envelope discussed above became a foundation for a reconstruction scheme based on Eq (1). Figure 4 illustrates the workflow of the reconstruction process. A guess of momentum spread and emittance is used to simulate diagnostics output. This output is compared to measurements and a difference between them is calculated. The guess is updated to minimize this difference. The cycle is repeated until desired difference level are achieved.

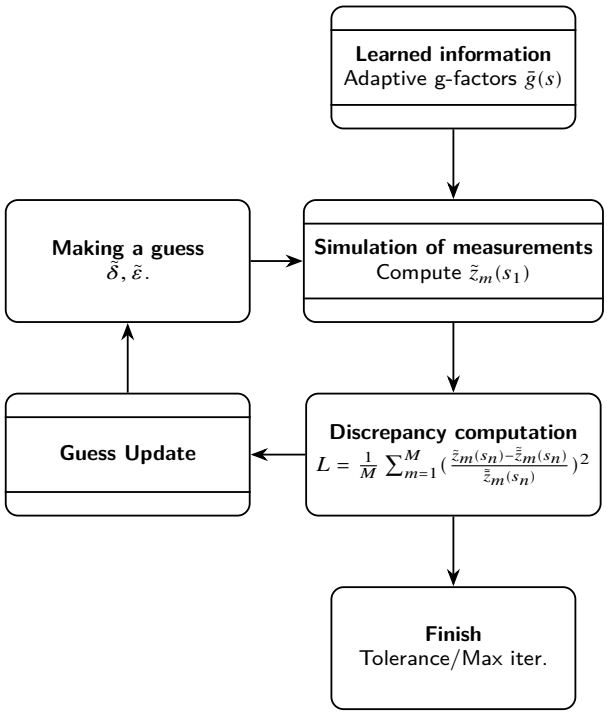

Figure 4: Phase space tomography algorithm. A guess of phase space distribution is used to simulate diagnostics output. This output is compared to measurements. The guess is updated to minimize loss function's value. The cycle is repeated until desired discrepancy level are achieved.

To test its performance we set ground truth values from [6] for emittance and momentum spread into a particle-tracking simulation and simulated profiles at positions s_0 and s_1. As a result, the scheme was able to reconstruct ground truth emittance and ground truth momentum spread with a 1% accuracy.

VOLTAGE OPTIMIZATION

Calculation of gradients allows us not only to use gradient descent algorithm in reconstruction, but perform automated machine tuning as well. We optimized settings of two buncher cavities in the TK beamline to minimize momentum spread of bunches injected into SIS18.

Figure 5 gives an example of two voltage optimization runs for 1 mA and 15 mA currents. This illustrates different roles of buncher cavities in a momentum spread minimizing beamline: the fist one serves a bunch as long as possible to maximize the efficiency of the second buncher, which minimizes the momentum spread. This explains why behavior of the first buncher voltage depends on current - intense bunches get elongated by their own space charge forces and the overall efficiency gets limited by nonlinear effects in the second cavity.

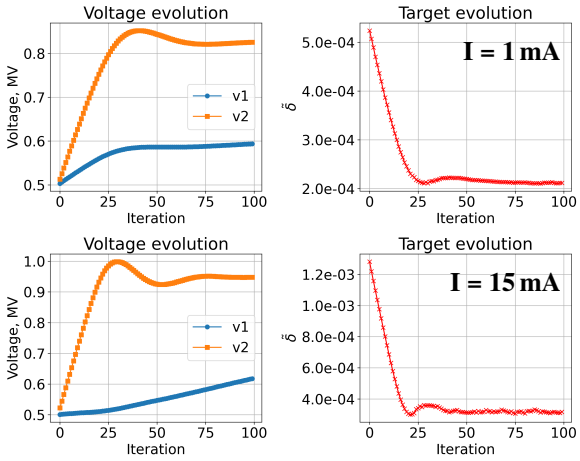

Figure 5: Voltage optimization runs for I =1 mA (top) and I =15 mA (bottom). Voltage settings of the second buncher reach a plateau with momentum spread, while settings of the first buncher continue to change. This indicates high sensitivity of $\tilde{\delta}$ to V_2 and a lower sensitivity to V_1 at high intensities.

On the optimization level this role difference is expressed in a low value of $\partial\tilde{\delta}/V_1$ at high beam intensities. This leads to a drift of V_1 without noticeable improvement of $\tilde{\delta}$.

SUMMARY

The phase space reconstruction at the GSI TK should provide the initial longitudinal bunch distribution provided by the UNILAC, using the bunch profiles measured by BSMs at two positions. An important application is the prediction and the minimization of the momentum spread for SIS injection, at the TK end.

A simulation model based on the longitudinal envelope equation with the adaptive g-factors was chosen to predict the bunch length along the TK. The model takes into account space-charge forces in a Gaussian profile approximation and cavity field nonlinearities.

The simulation model and the reconstruction scheme give the derivatives of all parameters and therefore also allows for the optimization of the buncher cavity settings, for minimum momentum spread.

ACKNOWLEDGMENTS

This work is supported by BMFTR project 05P24RD7

REFERENCES

[1] J. Stadlmann, L. Bozyk, P. Forck, D. Ondreka, R. Singh, and P. Spiller, "Sis18 operation and recent development", *Proc. IPAC'23*, pp. 1683–1686, 2023. doi:10.18429/JACoW-IPAC2023-TUPA163

[2] W. Barth, U. Scheeler, H. Vormann, M. Miski-Oglu, M. Vossberg, and S. Yaramyshev, "High brilliance beam investigations at the universal linear accelerator", *Phys. Rev. Accel. Beams*, vol. 25, no. 4, p. 040101, 2022. doi:10.1103/PhysRevAccelBeams.25.040101

[3] F. J. Sacherer, "Rms envelope equations with space charge", *IEEE Trans. Nucl. Sci.*, vol. 18, no. 3, pp. 1105–1107, 1971. doi:10.1109/TNS.1971.4326293

[4] M. Reiser, *Theory and design of charged particle beams*. John Wiley & Sons, 2008. doi:10.1002/9783527622047

[5] C. K. Allen, M. Reiser, and N. Brown, "Image effects for bunched beams in axisymmetric systems", *Part. Accel.*, vol. 45, pp. 149–165, 1994. https://cds.cern.ch/record/1108293

[6] L. Groening *et al.*, "Benchmarking of measurement and simulation of transverse rms-emittance growth", *Phys. Rev. Spec. Top. Accel. Beams*, vol. 11, no. 9, p. 094201, 2008. doi:10.1103/PhysRevSTAB.11.094201